Optics Communications 529 (2023) 129071

Contents lists available at ScienceDirect

Optics Communications

journal homepage: www.elsevier.com/locate/optcom

Design and analysis of passive and phase insensitive all-optical isolator in linear optical platform

Kamanashis Goswami [a], Haraprasad Mondal [a,b], Mrinal Sen [a,*]

[a] Electronics Engineering, Indian Institute of Technology (ISM) Dhanbad, Jharkhand, India
[b] Dibrugarh University Institute of Engineering and Technology, Dibrugarh University, Assam, 786004, India

ARTICLE INFO

Keywords:
Optical isolator
Photonic Crystal
Phase independent
Band diagram
Plane wave expansion
Finite difference time domain

ABSTRACT

In this work a very simple all-optical isolator, based on 2D holes in slab Photonic Crystal (PhC) waveguide, has been proposed and its performance has been investigated by Finite-Difference Time-Domain (FDTD) method. The unidirectional characteristic of the waveguide is phase independent in nature and no extra bias signal has been used. The structure is basically a 'W1' pyramid shaped waveguide having a 120° -bend in it and the unidirectional property has been achieved by making some structural modification in the bend region. This design is capable of providing a high forward transmittance of 72%, very low backward transmission of 10% and high contrast ratio 8.57 dB. Due to its simple structure, small footprint (416 μm^2), high forward transmission and high contrast ratio altogether make the isolator suitable for upcoming photonic integrated circuits.

1. Introduction

In the last few years, researchers have shown huge interest towards designing PhC based all optical logic gates and all optical logic devices due to the inherent abilities of PhC to control optical signals in sub-wavelength scale that play important role in photonic integrated circuit (PIC) design. Thereafter, as a result, several all-optical gates [1–6] and all optical devices like adder/subtractor [7–14], filter [15–17], demux [18,19], polarizer [20], decoder [21–27], coupler [28] etc have been reported in recent past, both in linear and non-linear domain. Several devices are fabricated in a PIC and those devices are connected by waveguides. Sometimes some parts/ individual devices are needed to be protected from unwanted optical back propagation which may damage the sensitive parts. Some phase sensitive devices also malfunction if any unwanted optical signal enters into the device. Optical isolator, also known as optical diode, is a solution for this problem. An optical isolator allows light to flow unidirectional i.e., it prevents optical signal from reflecting back toward the source. It also limits the optical noise. Therefore, it is highly recommendable to incorporate optical isolator circuit in next generation PIC to protect the highly photo/ phase sensitive inbuilt parts.

In this context, it is worth to mention that, few designs of non PhC based optical isolator [29,30] have also been reported in recent past where MZIs, polarizer, phase modulator, and/or sampler etc have been used. Though these designs offer very high contrast ratio, but the optical components used in those designs are having large footprint (in millimeter range). Hence, these designs are not suitable for next generation PICs. Y. Kawaguchi et al. [31] has proposed a design using spin-Hall effect of light in Ce:YIG film based magneto optic material and it provides a contrast ratio of 20 dB. Furthermore, D.D. Solnyshkov et al.. has also proposed one polariton graphene based topological optical isolator [32] which gives a tremendous contrast ratio, i.e., 49 dB. However, in spite of their excellent performance, fabrication of these aforesaid designs in silicon photonic based PICs is very much challenging because of the typicality of the used materials and their bulky size. On the other hand, PhC based designs are simpler to integrate as they are in line with conventional CMOS fabrication technologies that are used to design silicon based photonic and electronic devices.

Nonlinear PhC based designs [33,34] required very small footprint area and provide very high forward transmission as well. However, high input power (threshold power) is required for proper functioning of a nonlinear device. On the other hand, linear optical phenomena-based design is not constrained by a threshold power. Wang et al. [35] have designed an isolator in linear PhC within small footprint areas, but the forward power of the device is not sufficient enough. Moreover, the designs are purely two dimensional, i.e., the third dimension (normal to the periodic plane of the crystal) is considered as indefinitely extended, which is not at all practical. One isolator [36], based on linear PhC has been designed in a 3D PhC platform considering the third dimension having a finite height. But the rods in air structure makes the device mechanically weak and its fabrication process is bit challenging compare to holes in slab structure.

* Corresponding author.
E-mail addresses: kamanashis.goswami@gmail.com (K. Goswami), mandal.haraprasad@gmail.com (H. Mondal), mrinal.sen.ahm@gmail.com (M. Sen).

https://doi.org/10.1016/j.optcom.2022.129071
Received 12 July 2022; Received in revised form 30 September 2022; Accepted 12 October 2022
Available online 19 October 2022

To brief, Chen Wang et al. [37] have utilized the linear optical phenomena to design an on-chip small footprint optical diode/isolator based on a heterojunction silicon PhC slab. The heterojunction is made by forming two domains in a square lattice PhC slab, where both the domains have the same lattice constant but with different radii of their air holes. This heterojunction geometry breaks the symmetry in spatial inversion in the middle plane of the structure. The directional bandgap in this structure gets mismatched, which initiates unidirectional time-independent mode transitions. The device shows a forward transmittance in the order of 21.3% with a best-case contrast ratio of forward to backward transmittance of 0.885. Further, the research group has by designing a back-to-back optical diode [38] that shows a round-trip transmittance of merely 0.3% of the maximum forward transmittance, providing remarkable isolation. Nevertheless, its low forward transmittance debars its utility in most PIC applications.

On the other hand, S. Feng et al. [39] have proposed the design of an optical isolator exploiting the self-collimation phenomenon of the PhC. Their design consists of a heterojunction in the Γ-M direction, formed by two PhC sections arranged in a 2D square lattice having the same lattice constant. One of these PhCs is designed by an array of rectangular metal (here taken as Ag) rods on a silicon substrate, and the other is designed by circular holes perforating the silicon slabs. Simulation shows that the structure is able to provide a peak forward-transmittance of 60% and a backward transmittance of less than 0.1%. This is definitely a remarkable contrast ratio. However, it is quite challenging to fabricate the said heterostructure on silicon substrate due to their asymmetric designs (one PhC is made of rods and the other with air holes) and asymmetric materials (one material is Ag and the other is perforated silicon slab). Moreover, in a practical scenario, the design needs to be formed on a silicon slab, where the vertical positions in optical confinements in each of the PhC regions would have significant dissimilarity. It is expected that this dissimilarity would result in a significant difference in transmittance of the experimental outcome from that reported here, which are obtained through simulations. Therefore, the practical utility of this design in PICs also becomes also questionable.

Hence, this work proposes an isolator based on a finite thickness silicon PhC slab perforated by air holes arranged in a triangular lattice to obtain a better performance and practicality. Such a design is mechanically robust and more feasible in view of fabrication. The device is a star shape junction of three W1 wave guides. Unidirectional property of the proposed isolator has been achieved by making some simple structural modification in the junction region. The design dose not required any bias signal and its performance does not depend on the phase angle of the input signal. No nonlinear elements have been used, hence the proposed isolator removes the requirement of any threshold power. The holes in slab structure of the device makes it mechanically robust and bit simpler to fabricate. As the device consists of three L shape waveguide only, hence foot print area is not a big issue. It can be adjusted accordingly. Not the least, the reasonably good isolation (contrast ratio) isolator keeps it ahead of several designs in the context of its integration to silicon-based PICs.

The article is organized as follows. The next section details the design parameters of the proposed optical isolator. The band diagram of the non-defect photonic crystal, as well as its guided band diagram for the defect mode, has been presented and analyzed in the same section. Followed by the design procedure, the simulation results of the proposed device have been discussed in Section 3. Finally, the chapter presents a conclusion of the proposed work in the last section.

2. Architectural design of the device

The schematic of the proposed optical isolator is shown in Fig. 1. It has been designed using a PhC that is considered to be designed via perforating a silicon slab with air holes in regular periodic arrangements. The PhC consists of a hybrid interface formed by a square lattice and a triangular lattice section having the same lattice constant (say ‘a’). The slab has a finite thickness (i.e., 0.7a) and has been considered to be built in an air-bridge configuration to maintain its vertical symmetry.

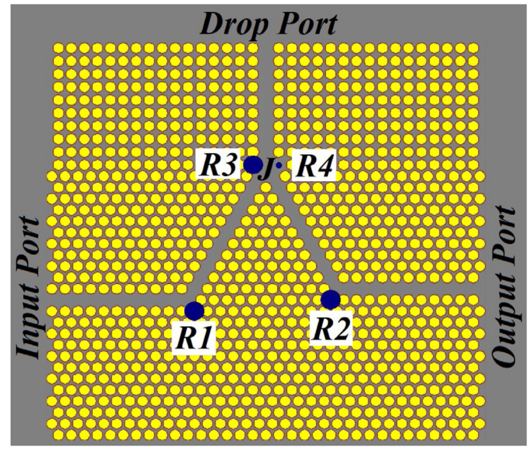

Fig. 1. Schematic representation of proposed optical isolator.

The lattice constant (a) has been taken as 500 nm, and the radius (r) of the air holes has been selected as 0.4a. The refractive index of the silicon slab is considered to be 3.46. However, in case of 2D equivalent analysis of a finite thickness slab, the effective index model better represents its 3D counterpart. The effective index of this slab is considered here as 3. The projected band diagram a W1 waveguide in the triangular lattice section and its transmittance are shown in Figs. 2(a) and (b), respectively. The same for a W1 waveguide in the square lattice have been shown, respectively, in Figs. 2(c) and (d). These figures show that both the structures support propagation of the targeted wavelength of 1550 nm (i.e., 0.322(a/λ)). The proposed isolator is basically a star connection of three W1 waveguides, as shown in Fig. 1. The junction of the three waveguides is at the interface of the heterostructure. Out of the three W1 waveguides forming the star, two are designed within the triangular lattice section along the Γ-M direction, whereas the other is formed in the square lattice in the Γ-X direction. The waveguide in the triangular lattice is used for the propagation of input and output signals, whereas the vertical waveguide is used as a drop port to channelize the unwanted signal from the output port. Two holes at the junction have been optimized by modifying their radius as 1.7r and 0.4r, as shown in Fig. 1, to direct the optical signal from the INPUT port to the OUTPUT port. At the same time, this optimization restricts any optical signal to flow from the OUTPUT to the INPUT port; rather, the signal is diverted toward the vertical drop port. This happens due to the asymmetry in the junction (formed by unequal radii of the optimized holes) when viewed from the INPUT and OUTPUT waveguides. The waveguides that connect the INPUT and OUTPUT ports to the junction include two 60-degree bends. The bend regions have also been optimized by changing the radius of one hole (following the same strategy as shown in the last chapter) from r to 1.5r at the outer side of the bend for maximum power transfer through the bend.

3. Simulation results and performance analysis

Simulation of the proposed device has been carried out by using the FDTD method to analyze its different metrics. A monochromatic continuous-wave (CW) of normalized frequency 0.322(a/λ) (corresponding to the 1550 nm wavelength) is used to operate the device. A CW optical signal of unity power has been applied at the input. When the optical signal from the INPUT port reaches the junction, it interacts with the R3 and R4 holes that direct the beam to the OUTPUT port. This is because the combination of the R3 and R4 holes at this junction can

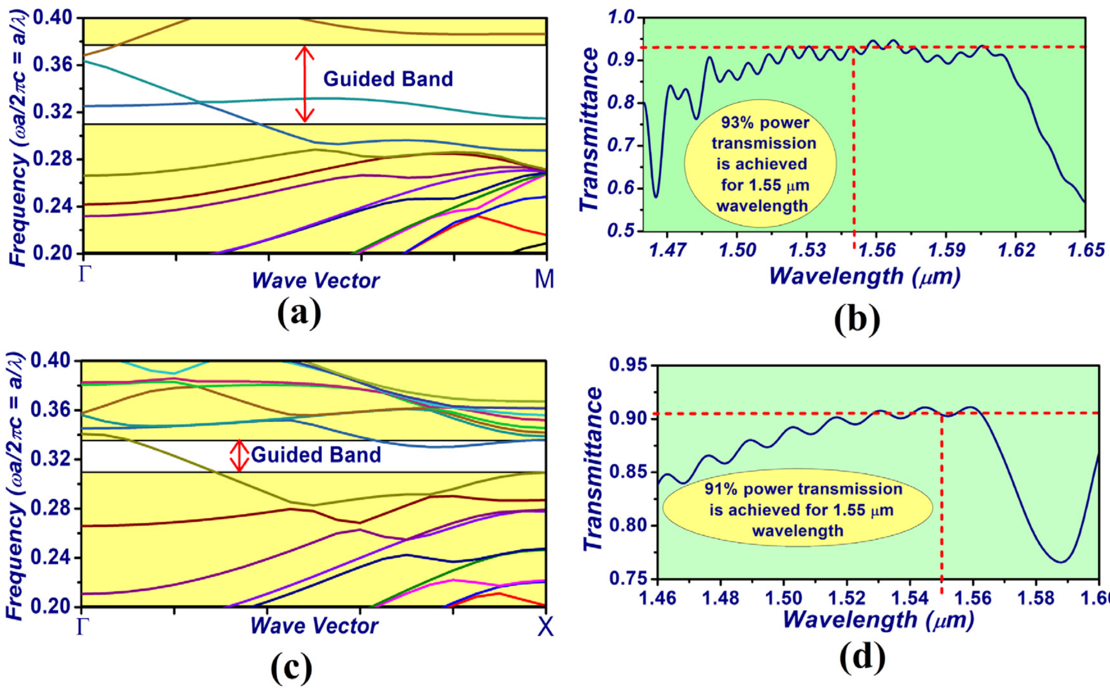

Fig. 2. (a) Projected band diagram and (b) Transmittance of a W1 waveguide in a triangular lattice, (c) and (d) are so in the square lattice.

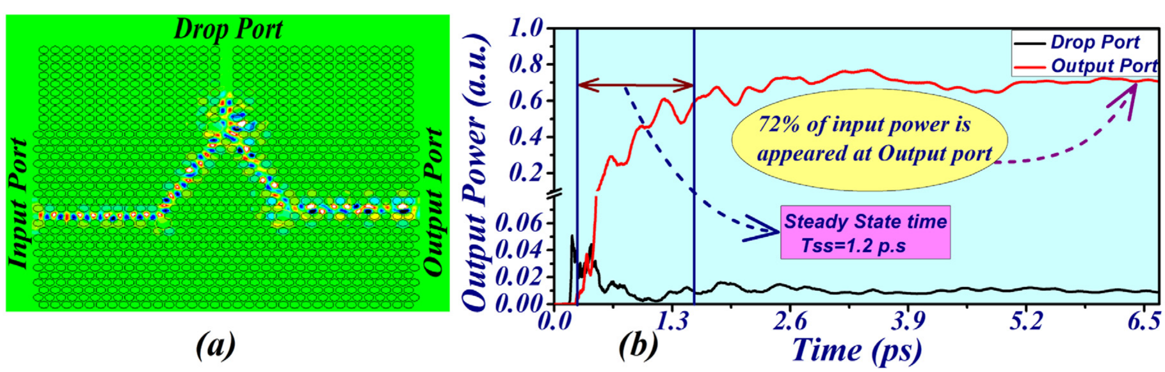

Fig. 3. (a) Field propagation and (b) power at OUPTUT port and DROP port when INPUT port is excited.

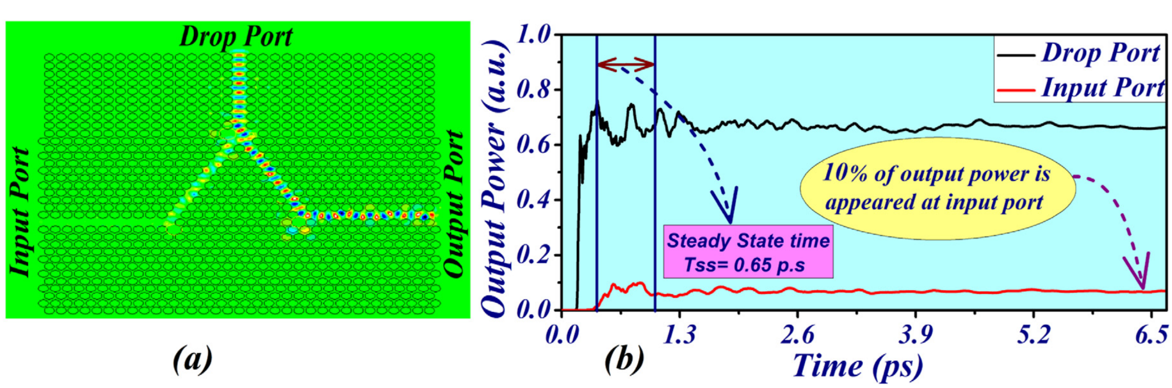

Fig. 4. (a) Field propagation and (b) power at INPUT port and DRAIN port when the OUTPUT port is excited.

be thought of as acting like a tiny reflector due to the index difference between the silicon waveguide and the holes. The concept can be understood from the ray-theory analogy. The electric field distribution of this state and the time-evolving power at the OUTPUT as well as the DROP port are shown in Figs. 3(a) and (b), respectively. The power of the output signal, in this case, is found as 72% (i.e., −1.43 dB) of the input. On the other hand, the same reflector combination reflects the optical beam coming from the OUTPUT port to the DROP port, restricting the wave propagation to the INPUT port. The electric field distribution of this state and the time-evolving power at the INPUT and DROP ports are shown in Figs. 4(a) and (b), respectively. This difference in the forward and backward transmission occurs due to the

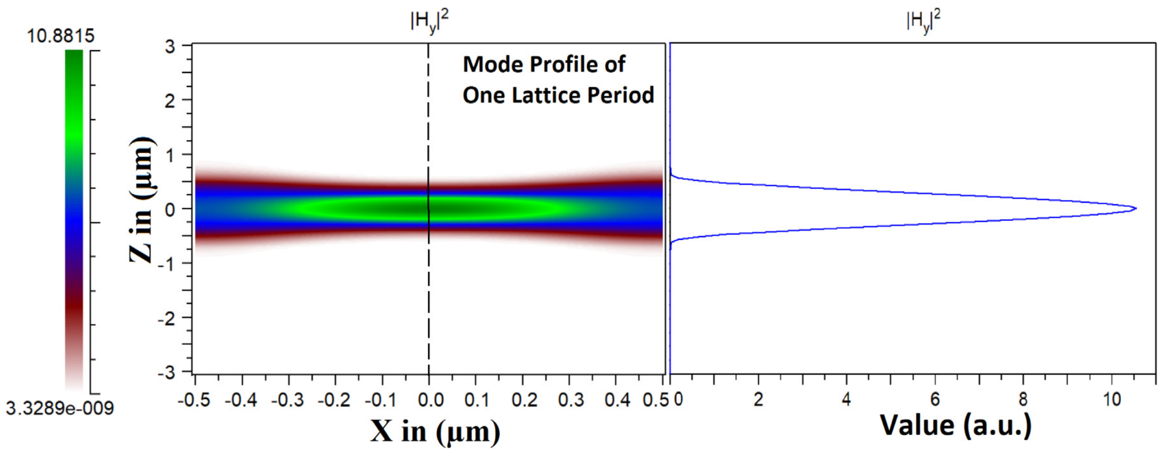

Fig. 5. Profile of even mode for one lattice period of square lattice.

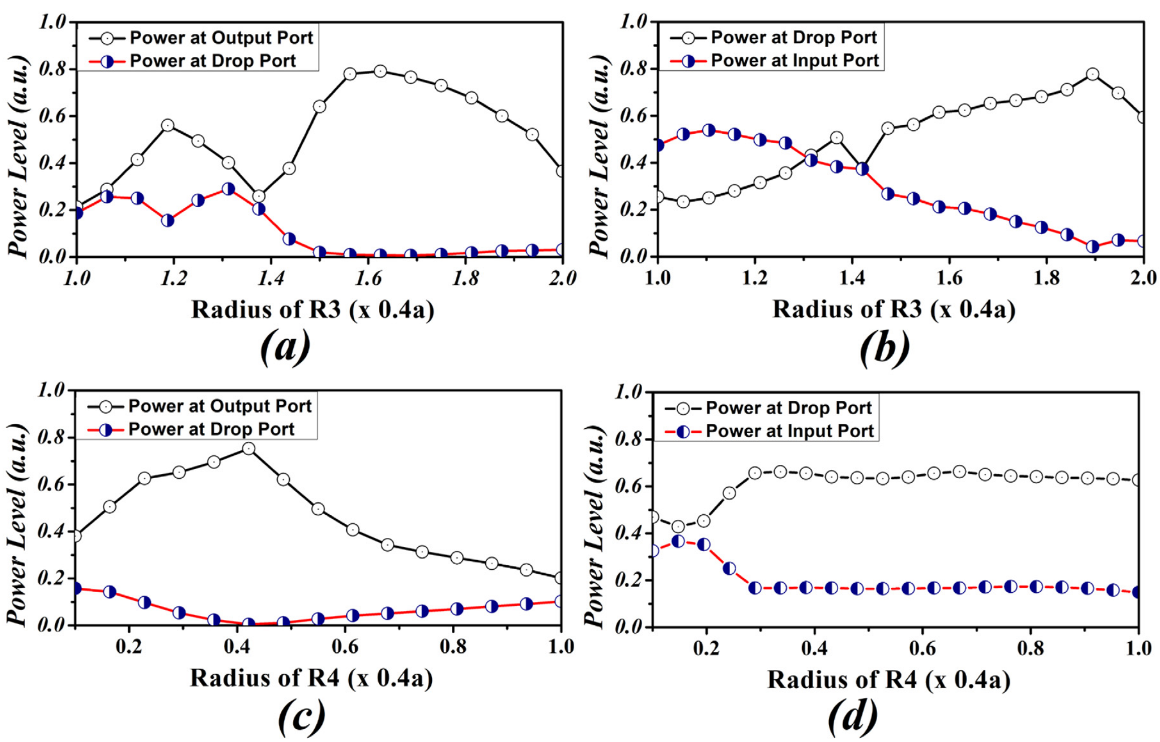

Fig. 6. Effect on (a) forward transmission and (b) backward transmission for variation of R3 and effect on (c) forward transmission and (d) backward transmission for variation of R4.

asymmetry of the junction when viewed from the different ports. As a result, the INPUT port receives only a small amount (10% or −10 dB) of the signal power that is launched from the OUTPUT port. These results indicate a contrast ratio of the forward to the reverse transmittance as 8.57 dB. It can be seen from the above Fig. 5 that the fundamental band is having a z-even profile that approximately matches with a Gaussian profile. However, when the wave launched from the input waveguide reaches the junction J (at the interface of the triangular and square lattice), the R3 and R4 creates a perturbation in the mode in such a way that it produces a higher order [40] Z-odd mode. But, the Z-odd mode propagation is not supported in the designed square lattice waveguide (the Drop port). Therefore, the wave experiences multiple destructive interferences with its reflected waves from the few successive PhC interfaces.

In this design, two holes in the junction region have been optimized by changing the radius of holes as 1.7r and 0.4r heuristically. After optimization the junction region looks asymmetric from INPUT end and OUTPUT end. Under this condition, when the optical signal is launched from INPUT port, the locally excited modes at the junction couples with the mode propagating from the INPUT port and the OUTPUT port. No modes couple with the DROP port. But if it is launched at OUTPUT port, the locally generated higher mode couple with DROP port and no signal should propagate towards INPUT port. However, the effect of the change in radius of each hole in the transmission towards OUTPUT and DROP port have been calculated. The results are attached herewith. However, the collective effect of the defect holes (1.7r and 0.4r) make the device work as an isolator. Fig. 6 shows the transmission in INPUT, OUTPUT and DROP port due to the variation of size of individual defect holes in the junction, for both forward and reverse propagation.

From the above discussion, it can be concluded that the device as a whole can be used as an optical isolator, which allows the optical propagation from the INPUT to OUTPUT port but restricts the back propagation from the OUTPUT to INPUT port. Additionally, the device, unlike the one that is proposed in [36], does not require a

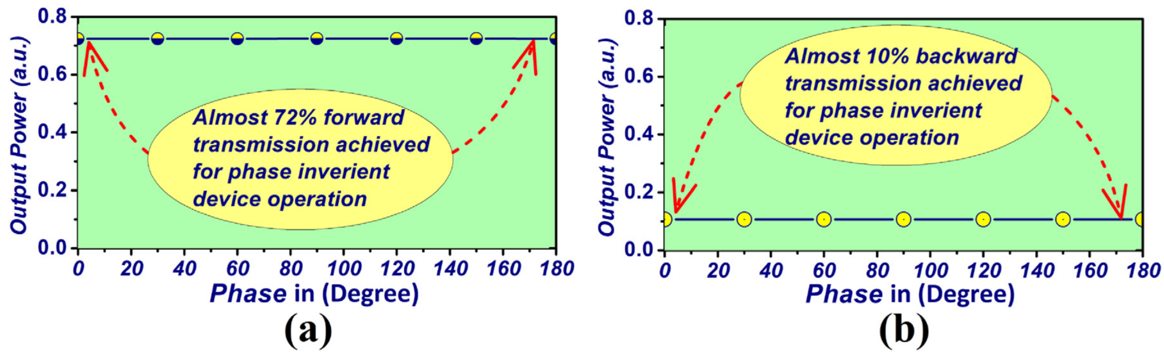

Fig. 7. (a) Forward and (b) backward transmittances at 1550 nm wavelength for different phase angle of the launched wave.

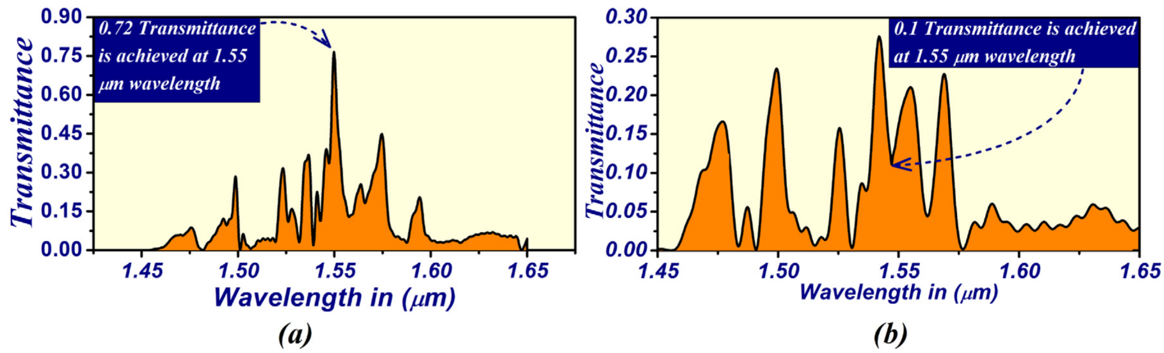

Fig. 8. (a) Forward transmittance spectrum and (b) backward transmittance spectrum.

bias signal and hence is a completely passive optical device. Another important property of the proposed isolator is that the device is purely phase-insensitive, which is, although intuitive but also been evaluated through simulation. In this simulation, the forward and reverse transmittances are evaluated for various phases of the launched signals. The results have been shown in Fig. 7, which corroborates the intuition of phase insensitivity of the device's operation. Therefore, the device can restrict the back propagation of the optical signal with any phase angle.

Further, the transmittance of the proposed isolator separately for the input and output excitations has also been calculated. Fig. 8(a) and (b) respectively show the forward and backward transmittance spectra of the proposed isolator. It can be seen from Fig. 8(a) that the maximum forward transmittance is obtained at the wavelength of 1550 nm. At this wavelength, the backwards transmittance is only 10%. Although Fig. 8 shows that the contrast ratio of the forward to backward transmittance is much high (∼14.4 dB) at the 1574 nm wavelength due to the very low backward transmittance (i.e., 1.6% or ∼18 dB), the forward transmittance is also reasonably low (i.e., 44.8% or 3.48 dB) and hence not used as the operating point. However, this operating point can be used in an application that needs better isolation by compromising the forward transmittance. Also, due to the scale invariability of PhC, the same design but with a suitable lattice constant may be chosen to map any of such operating points to any desired wavelength.

4. Conclusion

This work proposes a new design of an all-optical isolator based on a 2D square lattice holes-in-slab silicon-PhC structure. A hybrid PhC interface is formed by two PhC sections of same lattice constant, but while one has a triangular lattice the other is made in a square lattice arrangement. A star like junction is formed using three W1 waveguides. Two of these waveguides, forming the input and the output ports, are designed within the triangular lattice PhC at an angle 60° from each other. The third waveguide, called drop port, is formed with the square lattice PhC at an angle 150° from the other two ports. An asymmetry in viewing the junction from the input and the output ports is formed by modulating the radii of two holes at the star junction. This asymmetry results in directing the light from the input to the output port and so from output to the drop port. Thus, light in this device can pass from left port to the right port, but not the reverse, realizing the functionality of an isolator. The device has a footprint of 416 μm^2, and has been designed to operate at a wavelength of 1.55 μm. The forward and the reverse transmittance of the device have been observed to be −1.43 dB and −10 dB, respectively, at the designated wavelength. This results in a contrast ratio of forward to backward transmittance as 8.57 dB. Although these transmittances are reasonably good the bandwidth is found to be quite narrow. However, the small device footprint and passive operation (as is does not require a bias) make the device suitable for PIC applications.

Declaration of competing interest

The authors declare that they have no known competing financial interests or personal relationships that could have appeared to influence the work reported in this paper.

Data availability

No data was used for the research described in the article.

References

[1] A. Farmani, A. Mir, M. Irannejad, 2D-FDTD simulation of ultra-compact multifunctional logic gates with nonlinear photonic crystal, J. Opt. Soc. Amer. B 36 (4) (2019) 811–818.

[2] H. Mondal, S. Chanda, M. Sen, T. Datta, All-optical AND gate based on silicon photonic crystal, in: IEEE International Conference on Microwave and Photonics, Indian School Of Mines, Dhanbad, Jharkhand, 2015.

[3] H. Mondal, K. Goswami, M. Sen, W.R. Khan, Design and analysis of all-optical logic NOR gate based on linear optics, Opt. Quantum Electron. (2022) http://dx.doi.org/10.1007/s11082-022-03624-9.

[4] H.P. Mondal, M. Sen, C. Prakash, K. Goswami, C. Sarma, Impedance matching theory to design all-optical AND gate, IET Optoelectron. 12 (4) (2018) 244–248.
[5] K. Goswami, H.P. Mondal, P. Das, A. Thakuria, Realization of ultra-compact all-optical logic AND gate based on photonic crystal waveguide, ICCDN 2021, Lect. Notes Electr. Eng. 776 (2022) 61–68.
[6] H.P. Mondal, S. Chanda, P. Gogoi, Realization of all-optical logic AND gate using dual ring resonator, in: IEEE International Conference on Automatic Control and Dynamic Optimization Technique, ICACDOT-2016, 2016, pp. 553–556.
[7] Mohammad Mehdi Karkhanehchi, Fariborz Parandin, Abdulhamid Zahedi, Design of an all-optical half-adder based on 2D photonic crystals, Photonic Netw. Commun. 33 (2) (2017) 159–165.
[8] K. Goswami, H.P. Mondal, M. Sen, A review on all-optical logic adder: Heading towards next-generation processor, Opt. Commun. 483 (2020) 126668.
[9] Fariborz Parandin, Mohammad-Reza Malmir, Mosayeb Naseri, All-optical half-subtractor with low-time delay based on two-dimensional photonic crystals, Superlattices Microstruct. 109 (2017) 437–441.
[10] F. Parandin, M. Reza, Reconfigurable all optical half adder and optical XOR and AND logic gates based on 2D photonic, Opt. Quantum Electron. 52 (2020) 56.
[11] F. Cheraghi, M. Soroosh, G. Akbarizadeh, An ultra-compact all optical full adder based on nonlinear photonic crystal resonant cavities, Superlattices Microstruct. 113 (2018) 359–365.
[12] M.M. Karkhanehchi, F. Parandin, A. Zahedi, Design of an all-optical half-adder based on 2D photonic crystals, Photonic Netw. Commun. 33 (2017) 159–165.
[13] F. Parandin, M.R. Malmir, M. Naseri, All-optical half-subtractor with low-time delay based on two-dimensional photonic crystals, Superlattices Microstruct. 109 (2017) 437–441.
[14] M. Abdollahi, F. Parandin, A novel structure for realization of an all-optical, one-bit half-adder based on 2D photonic crystals, J. Comput. Electron. 18 (2019) 1416–1422.
[15] Haraprasad Mondal, Mrinal Sen, Kamanashis Goswami, Design and analysis of a 0.9Tb/s 6-channel WDM filter based on photonic crystal waveguides, J. Opt. Soc. Amer. B 36 (2019) 3181–3188.
[16] B.E. Olsson, P. Ohlen, L. Rau, D.J. Blumenthal, A simple and robust 40-Gb/s wavelength converter using fiber cross-phase modulation and optical filtering, IEEE Photonics Technol. Lett. 12 (2000) 846–848.
[17] M.P. Bulk, A.P. Knights, P.E. Jessop, et al., Optical filters utilizing ion implanted bragg gratings in SOI waveguides, Adv. Opt. Technol. (2008) 276165.
[18] H.P. Mondal, K. Goswami, M. Sen, C. Prakash, An all-optical ultra-compact 4-channel wavelength de-multiplexer, in: IEEE International Conference on Microwave and Photonics, Indian School of Mines, Dhanbad, Jharkhand, 2018.
[19] R. Talebzadeh, M. Soroosh, Y.S. Kavian, F. Mehdizadeh, Eight channel all-optical demultiplexer based on photonic crystal resonant cavities, Optik 140 (2017) 331–337.
[20] C. Prakash, M. Sen, H. Mondal, K. Goswami, Design and optimization of a TE-pass polarization filter based on a slotted photonic crystal waveguide, J. Opt. Soc. Amer. B 35 (8) (2018) 1791–1798.
[21] A. Sharma, K. Goswami, H.P. Mondal, T. Datta, M. Sen, A review on photonic crystal based all-optical logic decoder: Linear and nonlinear perspectives, Opt. Quantum Electron. 54 (2022) http://dx.doi.org/10.1007/s11082-021-03473-y.
[22] F. Mehdizadeh, M. Soroosh, H. Alipour-Banaei, A novel proposal for optical decoder switch based on photonic crystal ring resonators, Opt. Quantum Electron. 48 (2016) 20–29.
[23] F. Mehdizadeh, H.A. Banaei, S. Serajmohammadi, Design and simulation of all optical decoder based on nonlinear PhCRRs, Optik 156 (2018) 701–706.
[24] T. Daghooghi, M. Soroosh, K. Ansari, A low-power all optical decoder based on photonic crystal nonlinear ring resonators, Optik 174 (2018) 400–408.
[25] M.J. Maleki, M. Soroosh, A. Mir, Improving the performance of 2-to-4 optical decoders based on photonic crystal structures, Crystals 9 (12) (2019) 635–643.
[26] F. Mehdizadeh, H. Alipour-Banaei, S. Serajmohammadi, Study the role of non-linear resonant cavities in photonic crystal-based decoder switches, J. Modern Opt. 64 (2017) 1233–1239.
[27] H. Mondal, M. Sen, K. Goswami, Design andanalysis of all-optical 1 to 2 line decoder based on linear photonic crystal, IET Optoelectron. 13 (4) (2019) 191–195.
[28] C. Prakash, H. Mondal, K. Goswami, M. Sen, Investigation of optimum position of interface between strip waveguide and PhC slot waveguide for maximum power coupling, in: IEEE III International Conference on Microwave and Photonics, ICMAP 2018, Indian School of Mines, Dhanbad, Jharkhand, India, 2018, February 09–11 http://dx.doi.org/10.1109/ICMAP.2018.8354622.
[29] M.J.R. Heck, Grating coupler enabled optical isolators and circulators for photonic integrated circuits, IEEE J. Sel. Top. Quantum Electron. 21 (4) (2015) 361–369, 6100109 http://dx.doi.org/10.1109/JSTQE.2014.2385963.
[30] T. Mizumoto, Y. Shoji, Optical isolator with SOI waveguide, in: 2009 Conference on Optical Fiber Communication, 2009, pp. 1–3, http://dx.doi.org/10.1364/OFC.2009.OWV3.
[31] Y. Kawaguchi, M. Li, K. Chen, V. Menon, et al., Optical isolator based on chiral light-matter interactions in a ring resonator integrating a dichroic magneto-optical material, Appl. Phys. Lett. (2021).
[32] D.D. Solnyshkov, O. Bleu, G. Malpuech, Topological optical isolator based on polariton graphene, Appl. Phys. Lett. 112 (2018).
[33] A. Rostami, Piecewise linear integrated optical device as an optical isolator using two-port nonlinear ring resonators, Opt. Laser Technol. 39 (5) (2007) 1059–1065.
[34] S. Hua, J. Wen, X. Jiang, Q. Hua, L. Jiang, M. Xiao, Demonstration of a chip-based optical isolator with parametric amplification, Nat. Commun. 7 (2016) 13657.
[35] W. Chen, Z. Xiao-Lan, L. Zhi-Yuan, Linear and passive silicon optical isolator, Sci. Rep. 2 (1) (2012) 674.
[36] K. Goswami, H. Mondal, M. Sen, Design and analysis of all-optical isolator based on linear photonic crystal, Braz. J. Phys. 52 (78) (2022) 1–10.
[37] C. Wang, C.-Z. Zhou, Z.-Y. Li, On-chip optical diode based on silicon photonic crystal heterojunctions, Opt. Express 19 (27) (2011) 26948–26955.
[38] Z. Li, C. Wang, X. Zhong, Linear and passive silicon diodes, isolators, and logic gates, in: 2013 IEEE Photonics Society Summer Topical Meeting Series, 2013, pp. 189–190, http://dx.doi.org/10.1109/PHOSST.2013.6614451.
[39] S. Feng, C. Ren, W. Wang, Y. Wang, All-optical diode based on the self-collimation characteristics of the near-infrared photonic crystal heterojunctions, Europhys. Lett. (2012).
[40] P. Bettini, S. Boscolo, R. Specogna, M. Midrio, Design optimization of waveguide bends in photonic crystals, IEEE Trans. Magn. 45 (3) (2009) 1630–1633.